Progress In Electromagnetics Research M, Vol. 81, 67–73, 2019

A Broadband Optical Isolator Based on Chiral Plasmonic-Metamaterial Design

Andon Rangelov[1, *], Sotiris Droulias[2], and Vassilios Yannopapas[3]

Abstract—We theoretically propose a novel achromatic optical isolator based on circular dichroism in metamaterials of twisted chains of metallic nanoparticles. The suggested optical isolator consists of an input polarizer, followed by quarter-wave plate, then a circular dichroism material, another quarter-wave plate, and an output polarizer. In contrast to the most commonly used optical isolators, the current scheme does not use magnetic field and does not change the polarization plane.

1. INTRODUCTION

An optical diode, or optical isolator, is an optical device which allows light to travel in a single direction. These devices are typically used in optical communications and laser applications to protect a source from unwanted back reflections that might be damaging to optical tools. Furthermore, the use of an optical isolator usually improves the performance of an optical system as it suppresses instabilities and power spikes [1].

The first optical diode, with schematic shown in Figure 1, was proposed by Rayleigh [2] in 1885 with a simple design of two polarizers along with one Faraday rotator, which rotates the polarization of light by 45 degrees exploiting a magnetic-field induced circular anisotropy in the material (Faraday effect). However, Rayleigh's optical isolator has certain disadvantages. First of all, the design lacks broadband functionality as the rotation angle depends strongly on the wavelength while, at the same time, the rotation angle is proportional to the length of the Faraday rotator. One needs a very precise tuning of the light wavelength and Faraday-rotator length in order to achieve proper operation. A second drawback is that the magnetic field strength and Verdet constant exhibit temperature dependence. Moreover, the magnet is a major obstacle in downsizing the isolator so that it can be embedded in on-chip integrated systems. Additionally, due to the strong magnetic field around those isolators, no steel or magnetic objects should be brought close to them. An additional weakness is that Rayleigh's design alters the polarization of light through the optical isolator, for example, from vertical to 45 degrees polarization.

To overcome the magnetic issues, several ways have been proposed to realize optical isolators that do not use magneto-optical effects. Some of those approaches break time reversal symmetry in a different manner such as with the aid of the electro-absorption modulation [3], opto-acoustic effect [4], and phase modulation [5, 6]. More recently, a Mach-Zehnder-type modulator has been proposed [7]. In addition, a large class of optical isolators use nonlinear media to break Lorentz reciprocity [8–13].

In this paper, we propose a way to realize a broadband optical isolator which does not change the polarization plane based on a plasmonic-metamaterial design which consists of twisted chains of metallic nanoparticles. The approach is based on the effects of circular dichroism [14, 15] and nonreciprocal

Received 20 March 2019, Accepted 22 May 2019, Scheduled 22 May 2019

* Corresponding author: Andon Rangelov (rangelov@phys.uni-sofia.bg).

[1] Department of Physics, Sofia University, James Bourchier 5 blvd., Sofia 1164, Bulgaria. [2] Institute of Electronic Structure and Laser, FORTH, Heraklion, Crete 71110, Greece. [3] Department of Physics, National Technical University of Athens, Athens 15780, Greece.

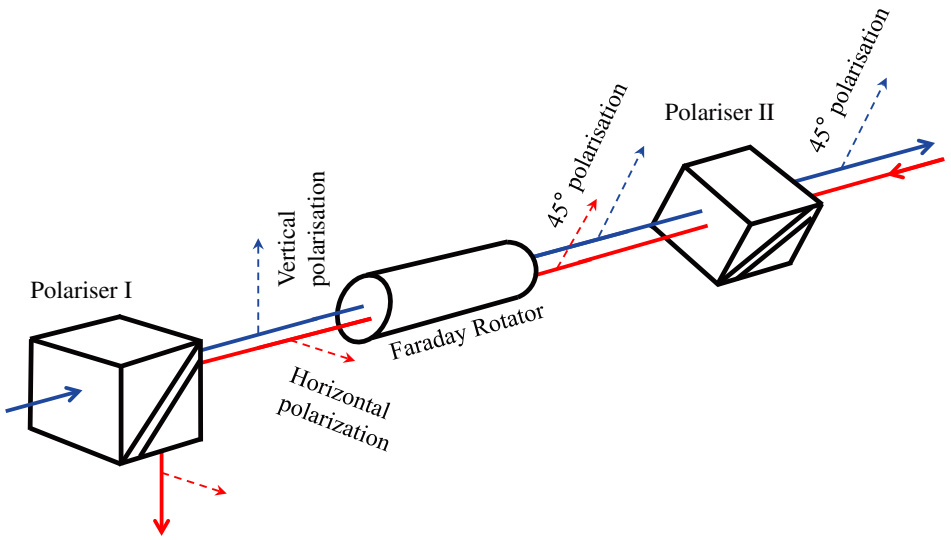

Figure 1. (Color online) Light traveling in the forward way (blue ray) becomes vertically polarized by polarizer I. The Faraday rotator rotates polarization by 45 degrees. The polarizer II then enables the light to pass through. Light traveling in the backward way (red ray) becomes polarized at 45 degree by polarizer II. The Faraday rotator will rotate the polarization by another 45 degrees (light is now polarized horizontally). Since the polarizer I is vertically aligned, the light will be blocked.

optical propagation. Our design combines advantages of other designs such as nonmagnetic realization of broadband optical isolation along with easy miniaturization so that it can be embedded in on-chip integrated systems. The miniaturization is favoured by the nanoscale design of the plasmonic metamaterial and the possible use of liquid-crystalline or Pockets-cell waveplates. In the latter case, a very fast switching probability is also within reach.

2. BROADBAND AND CIRCULAR-DICHROISM OPTICAL ISOLATOR

In our design, we have two quarter-wave plates (the first plate provides a retardance of $\pi/4$ with the second one $3\pi/4$), a material possessing strong circular dichroism [16], and two vertical polarizers at both end sides of our device. Figure 2 shows a schematic diagram of our design. After passing through the first polarizer light is vertically polarized. Then, it passes through the $\pi/4$ quarter-wave plate, and as a result the light polarization is altered to right circular polarization. After that, light passes unaffected through the circular-dichroism material (CD), which is designed to allow RCP waves to pass and blocks LCP waves. Next, light passes through the second quarter-wave plate (the one with $3\pi/4$ retardance) which transforms it from right circularly-polarized to vertically (linearly) polarized. Finally, the light passes without losses through the second polarizer. On its way back, the vertical polarized light is transformed to left circularly-polarized light after passing through the $3\pi/4$ quarter-wave plate, and it is eventually blocked by the CD material. Such a setup serves as an optical diode. If all elements in Figure 2 are broadband, then such an optical isolator operates within a wide spectral range. Since broadband quarter-wave plates and polarizers are available on market [17–19], we focus on how to realize a broadband and highly absorptive CD material. One obvious realization of a broadband CD setup is to use a stack of several layers of different materials with spectrally-shifted absorption maxima in the form of a multilayered composite material. A more efficient design, which we explore in the next section, is a plasmonic metamaterial which serves as a broadband and highly absorptive CD material.

3. PLASMONIC METAMATERIAL AS A CIRCULAR-DICHROISM MATERIAL

Next, we describe the plasmonic metamaterial which serves as a circular-dichroism material. The design we have in mind exhibits giant circular dichroism and can be viewed as a plasmonic analog

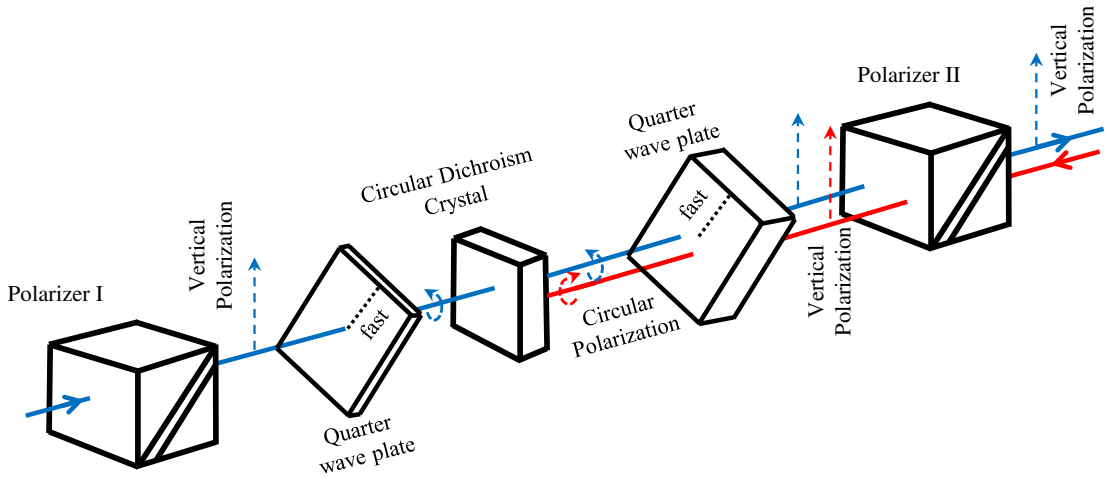

Figure 2. (Color online) Design of the broadband optical isolator. A vertical polarizer is followed by quarter-wave plate, a circular-dichroism material, a second quarter-wave plate and a second vertical polarizer. Light traveling in the forward direction (blue ray) becomes vertically polarized by polarizer I. The quarter-wave plate transforms incident light to right circularly-polarized which passes unaffected through the CD material. Then, it is converted once again to vertically polarized with the help of the second quarter-wave plate and finally passes through the polarizer II. Light traveling in the backward direction (red ray) becomes vertically polarized by polarizer II. Then the quarter-wave plate transforms it to left circularly-polarized which is eventually blocked by the circularly-dichroism material.

of twisted-nematic (cholesteric) liquid crystals [20, 21]. Namely, it is a two-dimensional (2D) array of chiral layer-by-layer meta-atoms consisting of mutually twisted linear chains of metallic nanoparticles (NPs), i.e., each layer of the meta-atom contains a linear chain of metallic NPs which is rotated relative to the preceding layer by a constant angle ϕ along the symmetry axis of the meta-atom (see Fig. 3). The optical properties of the chiral metamaterial under study are calculated by means of the discrete-dipole approximation (DDA), where each NP of the metamaterial is considered as a polarizable point dipole [16, 22–26]. The system is illuminated by either right or left (RCP/LCP) circularly polarized light, and solution of the corresponding DDA linear system of equations provides the scattered electric field. Then, the transmission, reflection, and absorption coefficients are calculated for each polarization, and the circular-dichroism (CD) is directly given by:

$$CD = 2\frac{A_{RCP} - A_{LCP}}{A_{RCP} + A_{LCP}}, \tag{1}$$

with A_{RCP} (A_{LCP}) being the absorption spectrum for right- (left-) circularly polarized light. The method described above is based on the local response approximation. However, since the nanoparticles in each chain are touching, quantum-effects can be taken into account for a refinement of the depicted absorption CD spectra [27].

The metamaterial is a 2D square array of the above three-dimensional (3D) meta-atom (see Fig. 4). The lattice of meta-atoms is described by the lattice vectors

$$\mathbf{R}_n = n_1\mathbf{a}_1 + n_2\mathbf{a}_2, \quad n_1, n_2 = -\infty \ldots + \infty \tag{2}$$

where $\mathbf{a}_1$ and $\mathbf{a}_2$ are the unit vectors of the 2D lattice of the metamaterial. The position of the ν-th NP (dipole) within a meta-atom (unit cell) is denoted by $\mathbf{R}_\nu$ where $\nu = 1, \ldots, N_m$ and N_m is the number of different NPs within the meta-atom.

The corresponding square-lattice unit vectors of 2 are provided by

$$\mathbf{a}_1 = a(1, 0), \quad \mathbf{a}_2 = a(0, 1) \tag{3}$$

where a is the 2D lattice constant. Each meta-atom is built up in a layer-by-layer fashion (see 3), i.e., a single layer lies in the xy-plane and consists of a linear chain of *touching* metallic NPs of radius S. The

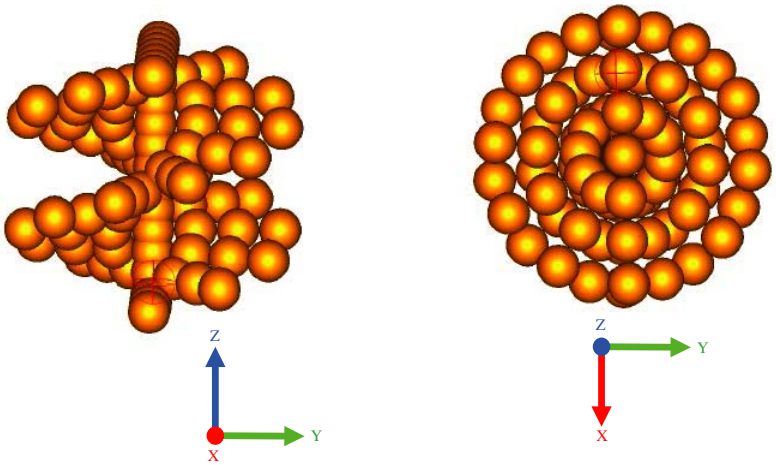

Figure 3. Side (left panel) and top (right panel) view of the meta-atom of the metamaterial design under study. The meta-atom consists of mutually twisted chains of metallic nanoparticles.

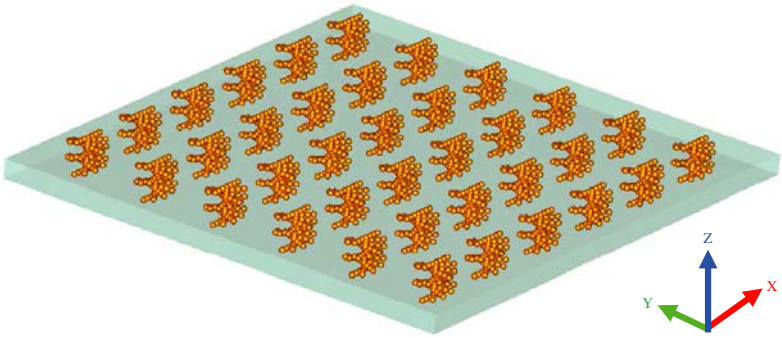

Figure 4. A square lattice of the meta-atoms of Fig. 3.

meta-atom consists of N_L layers, and each layer is indexed by $i = 1, \ldots, N_L$. The chain of NPs in each layer is rotated relative to the bottom (first) chain by an angle $\phi_i = 2\pi i/N_L$ (by angle $\Delta\phi = 2\pi/N_L$ relative to the previous chain). If each NP of a given chain is indexed by $j = 1, \ldots, N_C$ where N_C is the number of NPs in each chain, then the position vector $\mathbf{R}_\nu$ of a given NP within the meta-atom is provided by

$$\mathbf{R}_\nu = \mathbf{R}_{ij} = 2S(j\cos\phi_i, j\sin\phi_i, i) \quad j = 1, \ldots, N_C,\ i = 1, \ldots, N_L \tag{4}$$

Obviously, the total number of NPs within each meta-atom is $N_m = N_C \times N_L$ and the height $h = 2N_L S$.

We consider a twisted metamaterial (see Fig. 4) of gold NPs with radius $S = 5\,\text{nm}$ whose dielectric function is taken from experiment [28]. The meta-atom consists of $N_L = 11$ chains of NPs, mutually twisted by an angle $\Delta\phi = 2\pi/N_L = 2\pi/11\text{rad} = 32.73°$, wherein each chain consists of $N_C = 7$ NPs. The 2D lattice constant is $a = 4N_C S = 140\,\text{nm}$, and the height of the (chiral) meta-atom is $h = 2N_L S = 110\,\text{nm}$. The 2D surface coverage, i.e., the fraction of the xy-plane covered by a single chain of NPs is $f = N_C\pi(S/a)^2 = 2.8\%$. Fig. 5 shows the absorption circular-dichroism (CD) spectrum of the above twisted plasmonic metamaterial. It is obvious that there is broad spectral region, namely from 700–1000 nm where the absorption CD is remarkably high (50% on the average for this spectral region) serving the purpose of a CD material with broadband operation. We note that the particular choice of the geometrical parameters N_L and N_C provides an optimized metamaterial setup as it maximizes the range of the absorption CD spectrum. An in-depth parametrical study of the absorption CD spectrum as well as an explanation of the underlying physical mechanism can be found in [16].

Consequently, such a plasmonic-metamaterial design is ideally suited for the realization of

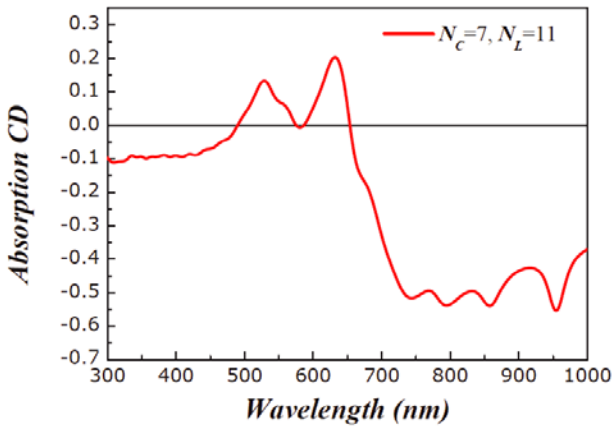

Figure 5. Absorption circular dichroism (CD) for a square lattice of twisted chains of 5nm NPs for $N_C = 7$ and $N_L = 11$. The 2D lattice constant is $a = 4N_C S = 140$ nm.

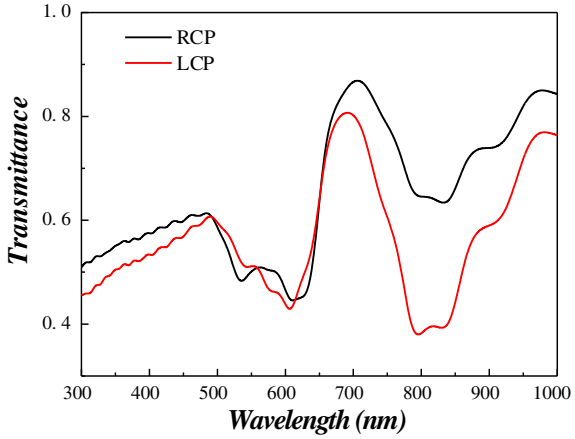

Figure 6. Spectrum of transmittance for left- (LCP) and right-(RCP) circularly polarized light for the square lattice of twisted chains of Fig. 5.

broadband optical isolator in the range between 700 nm and 1000 nm, based on the configuration of Figure 2. Since such a CD material possesses remarkably high absorption CD spectrum, one would expect that the isolation efficiency of such an optical isolator is equally high within a moderate range of isolator lengths. Also, in Fig. 6, we show the light transmittance for right- and left-circularly polarized light incident on the plasmonic metamaterial. We observe that for both polarizations (0.60 for the LCP and 0.70 for the RCP) the transmittance is sufficiently high for the proper operation of the proposed optical-isolator setup.

4. CONCLUSION

In this paper we have offered a simple means to realize a nonmagnetic and broadband optical isolator which competes with the standard magnetic setups. Our isolator design consists of two polarizers, two achromatic quarter-wave plates, and circular-dichroism material based on a chiral plasmonic metamaterial made of twisted chains of metallic nanoparticles. The expected transmission bandwidth of the suggested optical isolator is about 300 nm, which is the bandwidth of high absorption circular-dichroism of the chiral metamaterial. The suggested chiral metamaterial may be realized in the laboratory by suitable functionalization of gold nanoparticles with cholesteric liquid-crystal mesogens [29–31]. Finally, we should note that even though we suggest the operation of our broadband optical isolator with meta-materials of twisted chains of metallic nanoparticles, the scheme of operation is quite generic and may function with any material exhibiting similar broadband circular dichroism spectra. For example, in the THz regime, a suitable isolator design would comprise a superconducting THz metamaterial with huge nonlinearity and tenability [32].

ACKNOWLEDGMENT

A. Rangelov acknowledges support by the Bulgarian Science Fund Grant No. DN 18/14.

REFERENCES

1. Jalas, D., A. Petrov, M. Eich, W. Freude, S. Fan, Z. Yu, R. Baets, M. Popović, A. Melloni, J. D. Joannopoulos, M. Vanwolleghem, C. R. Doerr, and H. Renner, "What is and what is not an optical isolator," *Nat. Photonics*, Vol. 7, 579–582, 2013.

2. Rayleigh, L., "V. On the constant of magnetic rotation of light in bisulphide of carbon," *Phil. Trans. R. Soc. Lond*, Vol. 176, 343, 1885.
3. Ibrahim, S. K., S. Bhandare, D. Sandel, H. Zhang, and R. Noe, "Non-magnetic 30 dB integrated optical isolator in III/V material," *Electron. Lett.*, Vol. 40, 1293–1294, 2004.
4. Kang, M. S., A. Butsch, and P. St. J. Russell, "Reconfigurable light-driven opto-acoustic isolators in photonic crystal fibre," *Nat. Photonics*, Vol. 5, 549–553, 2011.
5. Doerr, C. R., N. Dupius, and L. Zhang, "Optical isolator using two tandem phase modulators," *Opt. Lett.*, Vol. 36, 4293–4295, 2011.
6. Doerr, C. R., L. Chen, and D. Vermeulen, "Silicon photonics broadband modulation-based isolator," *Opt. Express*, Vol. 22, 4493–4498, 2014.
7. Dong, P. and C. Gui, "Observation of nonreciprocal transmission in binary phase-shift keying modulation using traveling-wave Mach-Zehnder modulators," *Opt. Lett.*, Vol. 41, 2723–2726, 2016.
8. Trevino-Palacios, C. G., G. I. Stegeman, and P. Baldi, "Spatial nonreciprocity in waveguide second-order processes," *Opt. Lett.*, Vol. 21, 1442–1444, 1996.
9. Gallo, K., G. Assanto, K. R. Parameswaran, and M. M. Fejer, "All-optical diode in a periodically poled lithium niobate waveguide," *Appl. Phys. Lett.*, Vol. 79, 314, 2001.
10. Soljai, M., C. Luo, J. D. Joannopoulos, and S. Fan, "Nonlinear photonic crystal microdevices for optical integration," *Opt. Lett.*, Vol. 28, 637–639, 2003.
11. Lepri, S. and G. Casati, "Nonlinear photonic crystal microdevices for optical integration," *Phys. Rev. Lett.*, Vol. 106, 164101, 2011.
12. Fan, L., J. Wang, L. T. Varghese, H. Shen, B. Niu, Y. Xuan, A. M. Weiner, and M. Qi, "An all-silicon passive optical diode," *Science*, Vol. 335, 447–450, 2012.
13. Peng, B., S. K. Özdemir, F. Lei, F. Monifi, M. Gianfreda, G. L. Long, S. Fan, F. Nori, C. M. Bender, and L. Yang, "Parity-time-symmetric whispering-gallery microcavities," *Nature Phys.*, Vol. 10, 394–398, 2014.
14. Berova, N., K. Nakanishi, and R. W. Woody, *Circular Dichroism: Principles and Applications*, John Wiley & Sons, New York, 2000.
15. Shadrivov, I. V., V. A. Fedotov, D. A. Powell, Y. S. Kivshar, and N. I. Zheludev, "Electromagnetic wave analogue of an electronic diode," *New J. Phys.*, Vol. 13, 033025, 2011.
16. Droulias, S. and V. Yannopapas, "Electromagnetic wave analogue of an electronic diode," *J. Phys. Chem. C*, Vol. 117, 1130, 2013.
17. Eksmaoptics http://eksmaoptics.com/optical-components/polarizing-optics/retardation-plates-quartz-achromatic-wave-plates/.
18. Holmarc https://holmarc.com/beamsplitters.php.
19. Thorlabs https://www.thorlabs.com/.
20. Khoo, I. C., *Liquid Crystals*, Wiley, New Jersey, 2007.
21. Scharf, T., *Polarized Light in Liquid Crystals and Polymers*, Wiley, New Jersey, 2007.
22. Purcell, E. M. and C. R. Pennypacker, "Scattering and absorption of light by nonspherical dielectric grains," *Astrophys. J.*, Vol. 186, 705–714, 1973.
23. Draine, B. T., "Discrete-dipole approximation for scattering calculations," *J. Opt. Soc. Am. A*, Vol. 11, 1491–1499, 1994.
24. Flatau, P. J., "Improvements in the discrete-dipole approximation method of computing scattering and absorption," *Opt. Lett.*, Vol. 22, 1205–1207, 1997.
25. Yurkin, M. A. and A. G. Hoekstra, "The discrete dipole approximation: An overview and recent developments," *J. Quant. Spectrosc. Radiat. Transfer*, Vol. 106, 558–589, 2007.
26. Draine, B. T. and P. J. Flatau, "Discrete-dipole approximation for periodic targets: theory and tests," *J. Opt. Soc. Am. A*, Vol. 25, 2693–2703, 2008.
27. Tserkezis, C., M. A. T. Yesilyurt, J. S. Huang, and N. A. Mortensen, "Circular dichroism in nanoparticle helices as a template for assessing quantum-informed models in plasmonics," *ACS Photonics*, Vol. 5, 5017, 2018.

28. Johnson, R. B. and R. W. Christy, "Optical constants of the noble metals," *Phys. Rev. B*, Vol. 6, 4370, 1972.
29. Kanie, K., M. Matsubara, X. Zeng, F. Liu, G. Ungar, H. Nakamura, and A. Muramatsu, "Simple cubic packing of gold nanoparticles through rational design of their dendrimeric corona," *J. Am. Chem. Soc.*, Vol. 134, 808–811, 2011.
30. Bitar, R., G. Agez, and M. Mitov, "Cholesteric liquid crystal self-organization of gold nanoparticles," *Soft Matter*, Vol. 7, 8198, 2011.
31. Yu, C. H., C. P. J. Schubert, C. Welch, B. J. Tang, M. G. Tamba, and G. H. Mehl, "Design, synthesis, and characterization of mesogenic amine-capped nematic gold nanoparticles with surface-enhanced plasmonic resonances," *J. Am. Chem. Soc.*, Vol. 134, 5076–5079, 2012.
32. Kalhor, S., M. Ghanaatshoar, T. Kashiwagi, K. Kadowaki, M. J. Kelly, and K. Delfanazari, "Thermal tuning of high-Tc superconducting $Bi_2Sr_2CaCu_2O_{8+d}$ terahertz metamaterial," *IEEE Photonics Journal*, Vol. 9, No. 5, 1400308, 2017.